

Modeling Gravitational Waveforms from Stellar Encounters

Sophie Krisch

Department of Physics, Bucknell University, Lewisburg, PA 17837

This paper calculates the luminosity of gravitational waves emanating from close stellar encounters in both the classical limit and with first order post-Newtonian corrections. We also model gravitational waveforms with post-Newtonian corrections through the first order for varying eccentricities and angles of observation. Models are also generated using classical methods and are compared to those with post-Newtonian corrections. The stellar systems considered include bounded orbits with circular and elliptical trajectories as well as unbounded encounters such as parabolic and hyperbolic systems. We found that eccentricity has a much more pronounced effect on the shape of the gravitational waveform and the strain amplitude than the angle of observation, a dependence that is only introduced by post-Newtonian corrections.

INTRODUCTION

Gravitational wave (GW) research has advanced immensely since the first theoretical predictions of GWs by Einstein in 1916. Attempts to detect GWs has progressed from early resonant bar apparati to current laser interferometers such as VIRGO and LIGO. Recent advancements in instrumentation have lowered the frequency threshold of detectable GWs, and future projects such as Advanced LIGO promise a tenfold increase in sensitivity. Although GWs have still not been detected directly, indirect confirmations of Einstein's prediction, such as the shifting period of the Hulse-Taylor pulsar (PSR 1913+16) continue to fuel the search. Researchers hope to detect the first GWs when Advanced LIGO begins observations in 2013. In order to effectively sort through the vast amount of gravitational radiation detectors are expected to receive and classify the individual sources of many GWs superimposed into one signal, it is essential to understand what waveforms from various sources should look like. Analysis of GWs received by detectors will involve comparison of incoming signals to theoretically derived templates of gravitational waveforms from various astrophysical sources. This is particularly pertinent to the stochastic background, which is made up of many superimposed GW signals radiated from sources across the detector's field of view. Since the detector's angular resolution is much greater than the angular resolution of the GW sources, the detector receives a signal which is a mix of cosmological and astrophysical sources from uncorrelated GW emission events. Signal processing is being developed to efficiently break the stochastic signal into constituent waveforms, and comparing the resulting signals to theoretically generated templates should garner information about the events which contribute to the background radiation. Investigation of the stochastic background could provide information about the very early stages of the universe, much closer to the Big Bang than the analogous Cosmic Microwave background. For a more complete discussion of the stochastic microwave background and signal processing see [2] and [1].

In Section I, this paper generates a first approximation of gravitational waveforms from circular, elliptical, parabolic, and hyperbolic stellar encounters. These encounters are non-collisional interactions between two stars passing close by each other with either bounded (circular and elliptical) or unbounded orbits (parabolic and hyperbolic). Section II builds on the gravitational waveforms and luminosities calculated in Section I by including post-Newtonian corrections. The formalism used in Section II is based on initial work by Chandrasekhar, which was later applied to gravitational radiation by Epstein and Wagoner (1975). Post-Newtonian corrections add higher order terms to equations of motion, luminosity equations, and waveform equations to account for effects of relativity, radiation reaction, spin, and tidal effects. For example, equations of motion which include post-Newtonian corrections take the schematic form

$$\frac{d^2\mathbf{x}}{dt^2} = \frac{Gm\mathbf{x}}{r^3} \left[1 + O(\varepsilon) + O(\varepsilon^{\frac{3}{2}}) + O(\varepsilon^2) + O(\varepsilon^{\frac{5}{2}}) + \dots \right] \quad (1)$$

where the first term represents the classical Newtonian solution, and the various correction terms follow. Here we consider corrections to the $O(\varepsilon^2)$ order using results developed by Wagoner and Will (1976). While basic derivations of results pertinent to this paper are included, consult [6] for a more complete explanation. Inclusion of post-Newtonian corrections is important because improving the accuracy of waveform templates makes identification GW sources easier and improves the signal to noise ratio of GW detectors.

SECTION I

Newtonian Classifications of Stellar Orbits

This section treats the orbits of stars passing close to one another as classical Newtonian systems. This is a good first approximation for systems in which the orbiting bodies are compact objects. While very close encounters may in fact raise tidal forces which pull material from the surface of a star, consideration of this effect on GW waveforms is left to future research.

For two stars orbiting one another, of mass m_1 and m_2 , we represent the velocity of the first star, m_1 , as

$$v = v_r \hat{r} + v_\theta \hat{\theta} \quad (2)$$

where the radial velocity (v_r) is $v_r = \frac{dr}{dt}$, and the tangential velocity (v_θ) is $v_\theta = r \frac{d\theta}{dt}$. We now define two new parameters: the reduced mass ($\mu = \frac{m_1 m_2}{m_1 + m_2}$) and $\gamma = G m_1 m_2$. Considering the kinetic and gravitational potential energy, we can now write an equation for the energy of the entire system:

$$E = \frac{1}{2} \mu \left(\frac{dr}{dt} \right)^2 + \frac{L^2}{2\mu r^2} - \frac{\gamma}{r} \quad (3)$$

where the angular momentum (L) is

$$L = r^2 \frac{d\phi}{dt}. \quad (4)$$

We can also use Equation 3 to express the effective potential energy (V_{eff}),

$$V_{\text{eff}} = \frac{L^2}{2\mu r^2} - \frac{\gamma}{r} \quad (5)$$

At a certain radius (r_0), V_{eff} reaches a minimum value due to the interaction between the repulsive effects of the angular momentum term and the pull of the gravitational attraction term. Differentiating V_{eff} with respect to r we find that $r_0 = \frac{L^2}{\gamma\mu}$. Therefore, the minimum potential energy is

$$V_{\text{eff}} (\text{min}) = -\frac{\gamma^2 \mu}{2L^2} \quad (6)$$

Since the kinetic energy term is positive ($K = \frac{1}{2} \mu (\frac{dr}{dt})^2$), the total energy of the system cannot fall below V_{eff} . In the most extreme case, when the system's total energy is at a minimum, we can set $V_{\text{eff}} (\text{min}) = V_{\text{eff}}$ to solve for the maximum and minimum values of r .

$$r_{(\text{min}, \text{max})} = -\frac{\gamma}{2E} \pm \sqrt{\left(\frac{\gamma}{2E} \right)^2 + \frac{L^2}{2\mu E}} \quad (7)$$

Here the + corresponds to r_{max} and the - corresponds to r_{min} . Now we can solve the differential equation which gives the energy of the system (3) by defining a new variable $u = \frac{1}{r}$ and re-writing $\frac{dr}{dt}$ as

$$\frac{dr}{dt} = \frac{dr}{d\theta} \frac{d\theta}{dt} = \frac{L}{\mu r} \frac{dr}{d\theta} = \frac{-L}{\mu} \frac{1}{r} \frac{d}{d\theta}. \quad (8)$$

Making these substitutions in Equation 3 and dividing by $\frac{L^2}{2\mu}$ gives:

$$\frac{2\mu E}{L^2} = u'^2 + u^2 - \frac{2\mu\gamma}{L^2} u \quad (9)$$

where $u' = \frac{du}{d\theta}$. Differentiating with respect to θ gives

$$0 = u'(u'' + u - \frac{\gamma\mu}{L^2}), \quad (10)$$

which has the solutions $u' = 0$ and $u'' + u = \frac{\gamma\mu}{L^2}$. The first solution corresponds to circular orbits, while the second applies to all other possible conical orbits. The equation given by the second solution is made more clear by solving for u ,

$$u = \frac{\gamma\mu}{L^2} + C \cos(\phi + \alpha) \quad (11)$$

and then rewriting the expression in terms of the radius:

$$r = \left(\frac{\gamma\mu}{L^2} + C \cos(\phi + \alpha) \right)^{-1}. \quad (12)$$

Both C and α are integration constants from solving the differential equation (9), and since the solution (12) must satisfy the original equation (9), we can solve for C .

$$C^2 = \frac{2\mu E}{L^2} + \left(\frac{\gamma\mu}{L^2} \right)^2 \quad (13)$$

Plugging in the minimum energy (6), we find that $C \geq 0$. The value of C depends on the initial total energy of the system. The types of orbits which arise may be classified according to the initial energy and values of C as shown below.

TABLE I: Types of orbits resulting from initial energy conditions of the system.

C	E₀	Orbit Type
0	E_{min}	Circular
$0 < C < \frac{\gamma\mu}{L^2}$	$E_{min} < E < 0$	Elliptical
$ C = \frac{\gamma\mu}{L^2}$	0	Parabolic
$ C > \frac{\gamma\mu}{L^2}$	$E > 0$	Hyperbolic

Circular Orbits

In the case of binary systems with circular orbits, the radius of the orbit remains constant as a star precesses along the trajectory and ϕ (the angle from the center of the orbit to the star) changes. This means $u' = 0$ and consequently, $C = 0$, which eliminates the ϕ dependence in Equation 12. Using Equation 12 and the minimum energy equation (6) gives an expression for the radius of a stellar encounter with a circular orbit (r_0).

$$r_0 = \frac{\gamma}{2E_{min}} \quad (14)$$

Elliptical Orbits

In the case where C can take on a range of values from 0 to $\frac{\mu\gamma}{L^2}$, r depends on ϕ . Choosing $\alpha = 0$ puts the major axis of the ellipse along $\phi = 0$, and allows us to solve for the minimum and maximum values of r by using $\phi = 0$ and $\phi = \pi$ in Equation 12.

$$r_{min} = \left[\frac{\gamma\mu}{L^2} + C \right]^{-1} \quad (15)$$

$$r_{max} = \left[\frac{\gamma\mu}{L^2} - C \right]^{-1} \quad (16)$$

The semi major axis of the ellipse, a , is related to r by $2a = r_{min} + r_{max}$, so

$$a = \frac{\gamma\mu}{L^2} \left[\left(\frac{\gamma\mu}{L^2} \right)^2 + C^2 \right]^{-1}. \quad (17)$$

Or, using Equation 13 to eliminate C ,

$$a = \frac{\gamma}{2E}. \quad (18)$$

From basic geometric principles, the semi-latus rectum (l) is

$$l = \frac{L^2}{\gamma\mu}, \quad (19)$$

and using the general form of the radius of an ellipse $\frac{l}{r} = 1 + e \cos\phi$, we find that in this case r is

$$r = \frac{l}{1 + \epsilon \cos\phi}. \quad (20)$$

We define the eccentricity of the ellipse, ϵ , to be $\sqrt{\frac{1-l}{a}}$.

Parabolic and Hyperbolic Orbits

We can consider the parabolic and hyperbolic cases together, since the initial conditions on C and E give each unbounded orbits. For both cases r is still given by

$$r = \frac{l}{1 + \epsilon \cos(\phi)}, \quad (21)$$

but to ensure that r remains positive, ϕ must be restricted. Since $1 + \epsilon \cos(\phi) \geq 0$, $\cos(\phi) \geq -1$, and therefore $-\pi \leq \phi \leq \pi$. For a parabola, $\epsilon = 1$, so ϕ must remain between $-\pi$ and π . For a hyperbola, $\epsilon \geq 1$, which restricts ϕ to an even smaller range to meet the condition $\cos(\phi) \geq -1$. In both cases, r approaches ∞ as $\phi \rightarrow \pi$, which indicates the stars separate after the encounter.

Calculating GW Luminosity

Now that we have developed the equations for the trajectories of various orbits, we can use them to calculate the gravitational radiation emitted from each encounter. Using Einstein's weak field approximation, the metric is

$$g_{\mu\nu} = \delta_{\mu\nu} + \kappa h_{\mu\nu}, \quad (22)$$

and plane GWs are written as

$$h_{\mu\nu} = h e_{\mu\nu} \cos(\omega t - k \cdot x). \quad (23)$$

$e_{\mu\nu}$ is the unit polarization tensor of the wave, and a space-like, transverse wave travelling in the z direction can have two polarizations (e_1 and e_2).

$$e_1 = \frac{1}{\sqrt{2}}(\hat{x}\hat{x} - \hat{y}\hat{y}) \quad (24)$$

$$e_2 = \frac{1}{\sqrt{2}}(\hat{x}\hat{y} - \hat{y}\hat{x}) \quad (25)$$

Using the quadrupole approximation, in which the quadrupole mass tensor is given by

$$Q_{ij} = \sum_a m_a (3x_a^i x_a^j - \delta_{ij} r_a^2), \quad (26)$$

we can calculate the power radiated with

$$\frac{dE}{d\Omega} = \frac{G}{8\pi c^5} \left(\frac{d^3 Q_{ij}}{dt^3} e_{ij} \right)^2. \quad (27)$$

To find the total luminosity for both possible polarizations we add the luminosities of each polarization, plugging e_1 and e_2 into Equation 27. To simplify the total luminosity we use the conditions on the polarization tensor,

$$e_{\mu\nu} = e_{\nu\mu}, e_{\mu\mu} = 0, e_{\mu\nu}e_{\mu\nu} = 1. \quad (28)$$

The luminosity summed over the two polarizations gives

$$\sum_{pol} \frac{dE}{d\Omega} = \frac{G}{8\pi c^5} \left[\left(\frac{d^3 Q_{ij}}{dt^3} \right)^2 - 2n_i \frac{d^3 Q_{ij}}{dt^3} n_k \frac{d^3 Q_{kj}}{dt^3} - \frac{1}{2} \left(\frac{d^3 Q_{ii}}{dt^3} \right)^2 + \frac{1}{2} \left(n_i n_j \frac{d^3 Q_{ij}}{dt^3} \right)^2 + \frac{d^3 Q_{ii}}{dt^3} n_j n_k \frac{d^3 Q_{jk}}{dt^3} \right], \quad (29)$$

where the n is the unit vector describing the direction of the incoming radiation. To get the total luminosity of the incoming GWs we integrate over all directions of n (see [5] for further explanation). The total radiation received is

$$\frac{dE}{d\Omega} = \frac{G \langle Q_{ij}^{(3)} Q^{(3)ij} \rangle}{45c^5}. \quad (30)$$

The notation $Q_{ij}^{(3)}$ represents the third derivative of Q_{ij} with respect to time, and $\langle Q_{ij}^{(3)} Q^{(3)ij} \rangle$ indicates an average of the quadrupole mass tensors over several wavelengths. This average is necessary because it is impossible to pinpoint whether the energy of a GW lies in a particular crest or trough, and energy is described by relative displacements of objects rather than a single point in space. To evaluate the luminosity of GWs from stellar interactions, I first calculated each component of the quadrupole mass tensor in the plane of orbit (where $\theta = \frac{\pi}{2}$) using the relationships between Cartesian and spherical coordinates, $(x, y, z) = (r \cos(\phi) \sin(\theta), r \sin(\phi) \sin(\theta), r \cos(\theta))$.

$$\begin{aligned} Q_{xx} &= \mu r^2 (3 \cos^2(\phi) - 1) \\ Q_{yy} &= \mu r^2 (3 \sin^2(\phi) - 1) \\ Q_{zz} &= \mu r^2 \\ Q_{xz} &= Q_{zx} = 0 \\ Q_{yz} &= Q_{zy} = 0 \\ Q_{xy} &= Q_{yx} = 3\mu r^2 \cos(\phi) \sin(\phi) \end{aligned} \quad (31)$$

Circular and Elliptical Orbits

To find the GW luminosity of circular and elliptical stellar encounters I first used Equation 20 to find the angular velocity, $\dot{\phi}$. Substituting the radius of the ellipse (20) and l (19) into Equation 4, which relates $\dot{\phi}$ to angular momentum and radius, gives L in terms of G , l , m_1 , m_2 , and e :

$$\dot{\phi} = \frac{\sqrt{Gl(m_1 + m_2)}(e \cos(\phi) + 1)^2}{l^2}. \quad (32)$$

Using this result we can find the third derivatives of each quadrupole component:

$$\begin{aligned} \frac{d^3 Q_{xx}}{dt^3} &= \beta(24 \cos(\phi) + e(9 \cos(2\phi)) + 11) \sin(\phi) \\ \frac{d^3 Q_{yy}}{dt^3} &= -\beta(24 \cos(\phi) + e(13 + 9 \cos(2\phi))) \sin(\phi) \\ \frac{d^3 Q_{zz}}{dt^3} &= -2\beta e \sin(\phi) \\ \frac{d^3 Q_{xy}}{dt^3} &= -\frac{3}{2} \frac{(Gl(m_1 + m_2))^{\frac{3}{2}} \mu}{l^4} \end{aligned} \quad (33)$$

$$(1 + \cos(\phi))^2 (5e \cos(\phi) + 8 \cos(2\phi) + 3e[3\phi]) \quad (34)$$

where

$$\beta = \frac{Gl(m_1 + m_2)^{3/2} \mu (e \cos(\phi) + 1)^2}{l^4}. \quad (35)$$

Next I calculated the product $Q_{ij}^{(3)} Q^{(3)ij}$ by using the quadrupole components (34) to construct the matrix $Q_{ij}^{(3)}$ and then multiplying by the transpose. Substituting the resulting product,

$$Q_{ij}^{(3)} Q^{(3)ij} = \frac{G^3}{l^5} [(m_1 + m_2)^3 \mu^2 (\epsilon \cos(\phi) + 1)^4 (9(5\epsilon \cos(\phi) + 8 \cos(2\phi) + 3\epsilon \cos(3\phi))^2 + 4(11 + 24 \cos(\phi) + 9 \cos(2\phi))^2 \sin^2(\phi))] \quad (36)$$

into Equation 30, we find the total luminosity of circular and elliptical encounters:

$$\frac{dE}{d\Omega} = \frac{G^4 f(\phi)}{180 l^5 c^5}, \quad (38)$$

where

$$f(\phi) = [(m_1 + m_2)^3 \mu^2 (1 + \epsilon \cos(\phi))^4 (9(5\epsilon \cos(\phi) + 8 \cos(2\phi) + 3\epsilon \cos(3\phi))^2 + 4(11 + 24 \cos(\phi) + 9 \cos(2\phi))^2 \sin^2(\phi))] \quad (39)$$

To find the total radiation received over the entire length of the stellar interaction, integrate the instantaneous radiation received over time, or alternatively over ϕ .

$$\Delta E = \frac{G^5}{1440 l^5 c^5} \int_{\phi_1}^{\phi_2} f(\phi) d\phi. \quad (40)$$

For ϕ between 0 and π , the total energy emitted is

$$\Delta E = \frac{G^4 \pi (m_1 + m_2)^3 \mu^2}{1440 c^5 l^5} F(e) \quad (41)$$

where

$$F(\epsilon) = (m_1 + m_2)^3 \mu^2 \pi^2 (6912 + \epsilon(2592 + \epsilon(49216 + \epsilon(7776 + \epsilon(1296 + 1145\epsilon))))). \quad (42)$$

Since $F(\epsilon)$ only depends on the eccentricity, the amount of radiation emitted from a stellar encounter only depends on the initial conditions of the binary system.

Parabolic and Hyperbolic Orbits

Using the same techniques as in the elliptical case, we find the angular velocity for parabolic and hyperbolic orbits,

$$\dot{\phi} = l^2 L (\epsilon \cos(\phi) + 1)^2 \quad (43)$$

and the third derivatives of the quadrupole mass tensor, $Q_{ij}^{(3)}$

$$\begin{aligned} \frac{d^3 Q_{xx}}{dt^3} &= \rho(24 \cos(\phi) + \epsilon(9 \cos(2\phi)) + 11) \sin(\phi) \\ \frac{d^3 Q_{yy}}{dt^3} &= -\rho(24 \cos(\phi) + \epsilon(13 + 9 \cos(2\phi)) \sin(\phi) \\ \frac{d^3 Q_{zz}}{dt^3} &= -2\rho \epsilon \sin(\phi) \\ \frac{d^3 Q_{zz}}{dt^3} &= -\frac{3}{2} \rho (\epsilon \cos(\phi) + 1)^2 (5\epsilon \cos(\phi) \\ &\quad + 8 \cos(2\phi) + 3\epsilon \cos(3\phi)) \end{aligned} \quad (44)$$

where

$$\rho = l^8 L^3 \mu (\epsilon \cos(\phi) + 1)^2. \quad (46)$$

Using Equation 40 and Equation 45 as before gives the power radiated from parabolic and hyperbolic encounters:

$$\frac{dE}{dt} = \frac{G\rho^2}{15c^5} [912 + 125\epsilon^2 + 528\epsilon \cos(\phi) + 48(4 + 3\epsilon^2) \cos(2\phi) + 9\epsilon(16 \cos(3\phi) + 3 \cos(4\phi))] \sin^2(\phi), \quad (47)$$

or

$$\frac{dE}{dt} = \frac{Gl^{16}L^6\mu^2}{15c^5}f(\phi), \quad (48)$$

where $f(\phi)$ is now

$$f(\phi) = [912 + 125\epsilon^2 + 528\epsilon \cos(\phi) + 48(4 + 3\epsilon^2) \cos(2\phi) + 9\epsilon(16 \cos(3\phi) + 3 \cos(4\phi))] \sin^2(\phi) \quad (49)$$

Next we find the total radiation emitted during the interaction by using Equation 40 where $-\pi \leq \phi \leq \pi$, yielding

$$\Delta E = \frac{2Gl^{16}L^6\mu^2\pi}{15c^5}F(\epsilon), \quad (50)$$

where

$$F(\epsilon) = (1 + \epsilon \cos[\phi])^4(192 + 125\epsilon^2 + 528\epsilon \cos(\phi) + 48(4 + 3\epsilon^2) \cos(2\phi) + 9\epsilon(16 \cos(3\phi) + 3\epsilon \cos(4\phi))) \sin^2(\phi). \quad (51)$$

Repeating for the hyperbola, where $-\frac{3\pi}{4} \leq \phi \leq \frac{3\pi}{4}$, we find the total energy emitted during the interaction is:

$$\Delta E = \frac{Gl^{16}L^6\mu^2\pi}{10c^5}F(\epsilon), \quad (52)$$

where

$$F(\epsilon) = (1 + \epsilon \cos(\phi))^4(192 + 125\epsilon^2 + 528\epsilon \cos(\phi) + 48(4 + 3\epsilon^2) \cos(2\phi) + 9\epsilon(16 \cos(3\phi) + 3\epsilon \cos(4\phi))) \sin^2(\phi). \quad (53)$$

As in the elliptical system, $F(\epsilon)$ and the total energy radiated depend only on the initial dynamics of the stellar system.

Modeling the GW Waveforms

To model the gravitational waveforms we use the quadrupole mass tensors previously derived in the equation for the strain amplitude (h_{ij}):

$$h_{ij}(t, R) = \frac{2G}{Rc^4}\ddot{Q}^{jk}. \quad (54)$$

Here R is the distance from the source of the GWs to the observer, and the indices j, k run over 1, 2.

Elliptical Orbits

To find the GW amplitudes for an elliptical system, we use the quadrupole mass tensor components (31) and angular momentum (32) to find the necessary components of \ddot{Q}^{jk} to calculate strain (54). The individual components contributing to the total strain amplitude of the GWs are:

$$\begin{aligned} h^{11} &= \frac{-G^2\mu(m_1 + m_2)}{lRc^4}(13\epsilon \cos(\phi) + 12 \cos(2\phi) + \epsilon(4\epsilon + 3 \cos(3\phi))) \\ h^{22} &= \frac{G^2\mu(m_1 + m_2)}{lRc^4}(17\epsilon \cos(\phi) + 12 \cos(2\phi) + \epsilon(8\epsilon + 3 \cos(3\phi))) \\ h^{12} &= \frac{-6G^2\mu(m_1 + m_2)}{lRc^4}(4 \cos(\phi) + \epsilon(3 + \cos(2\phi))) \sin(\phi) \end{aligned} \quad (55)$$

Adding each component in quadrature, gives the total strain amplitude for the GW:

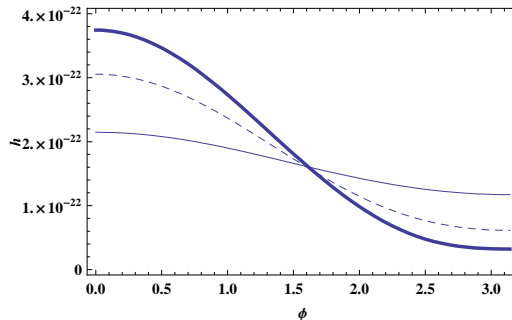
$$h = 2\sqrt{2} \left[\frac{G^4(m_1 + m_2)^2\mu^2}{l^2Rc^8}(36 + 59\epsilon^2 + 10\epsilon^4 + \epsilon(108 + 47\epsilon^2) \cos(\phi) + 59\epsilon^2 \cos(2\phi) + 9\epsilon^2 \cos(3\phi)) \right]^{1/2}. \quad (56)$$

To model these waveforms for a typical close stellar encounter we use the parameters in Table II.

We define one star, m_2 , to be at rest in relation to m_1 , which is moving with the velocity v_0 . When the stars reach the point of closest approach, the radial velocity of m_1 as seen by m_2 is 0, which allows us to fix the angular momentum as $L = bv_0$. Using the parameters in Table II, we can plot the waveforms for the various initial conditions and eccentricities representing different orbit shapes. The resulting waveforms for elliptical orbits with eccentricities $\epsilon = 0.2, 0.5, 0.7$ are shown below.

TABLE II: Parameters Used to Model a Close Stellar Encounter.

Parameter	Value	Units	Meaning
b	1	AU	Impact parameter
v_0	200	km/s	Initial velocity of m_1 relative to m_2
$m_1 = m_2$	$1.4 M_\odot$	kg	Masses of stars
R	8	kpc	Distance from encounter to observer

FIG. 1: Gravitational waveforms for elliptical orbits with varying eccentricities. The thick line represents $\epsilon = 0.7$, the dashed line is $\epsilon = 0.5$, and the thin line is $\epsilon = 0.2$.

Parabolic and Hyperbolic Orbits

Repeating the procedure for calculating the components of the strain amplitude, but using the angular momentum for the parabolic and hyperbolic cases (43) gives:

$$\begin{aligned}
 h^{11} &= \frac{-G\mu l^6 L^2}{Rc^4} (13\epsilon \cos(\phi) + 12 \cos(2\phi) + \epsilon(4\epsilon + 3 \cos(3\phi))) \\
 h^{22} &= \frac{G\mu l^6 L^2}{Rc^4} (17\epsilon \cos(\phi) + 12 \cos(2\phi) + \epsilon(8\epsilon + 3 \cos(3\phi))) \\
 h^{12} &= \frac{-6G\mu l^6 L^2}{Rc^4} (4 \cos(\phi) + \epsilon(3 + \cos(2\phi))) \sin(\phi)
 \end{aligned}
 \tag{57}$$

Adding each component in quadrature gives the total strain amplitude for the GW:

$$h = 2\sqrt{2} \left[\frac{G^2 l^{12} L^4 \mu^2}{R^2 c^8} (36 + 59\epsilon^2 + 10\epsilon^4 + \epsilon(108 + 47\epsilon^2)(\phi) + 59\epsilon^2(2\phi) + 9\epsilon^2(3\phi)) \right]^{1/2}. \tag{58}$$

For parabolic orbits we find that the waveform for the eccentricity $\epsilon = 1$ is

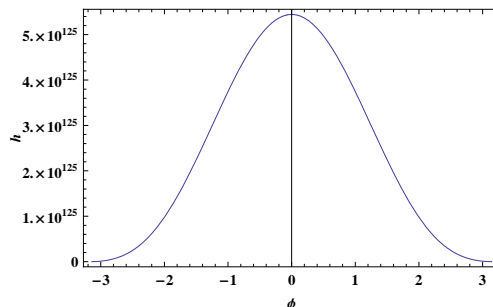


FIG. 2: Gravitational waveform of parabolic orbits with an eccentricity of 1.

For hyperbolic orbits we find that the waveforms for the eccentricities $\epsilon = 1.2, 1.5, 1.7$ are

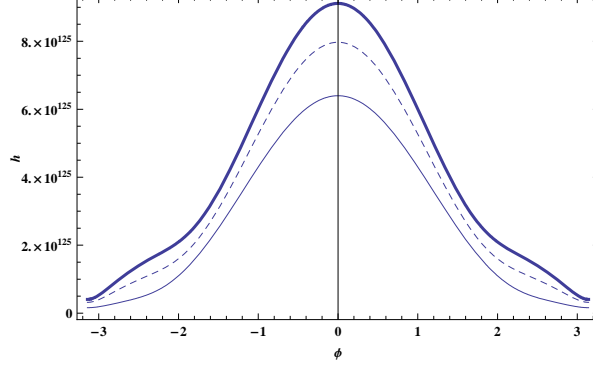


FIG. 3: Gravitational waveforms of hyperbolic orbits. The thick line represents eccentricity $\epsilon = 1.7$, the dashed line $\epsilon = 1.5$, and the thin line $\epsilon = 1.2$.

SECTION II

Calculating GW Luminosity

The luminosity of GWs emanating from a close encounter of two stars has the general form

$$L = \frac{R^2}{32\pi} \int \left\langle \left(\frac{\partial h_{TT}^{ij}}{\partial t} \right)^2 \right\rangle d\Omega, \quad (59)$$

where h_{TT}^{ij} is the transverse traceless component of the strain amplitude for two body systems. h_{TT}^{ij} including post-Newtonian corrections is given by:

$$\begin{aligned} h_{TT}^{ij} = & \frac{2\mu}{R} \left[2(v^i v^j - \frac{mr^i r^j}{r^3}) + \frac{\mu}{m} \left[(\mathbf{n} \cdot \mathbf{r}) \frac{3m}{r^3} (2v^{(i} v^{j)}) - \frac{\dot{r} r^i r^j}{r} \right] - (\mathbf{n} \cdot \mathbf{v}) (2v^i v^j - \frac{mr^i r^j}{r^3}) \right] \\ & + \frac{m}{3r} (1 - \frac{6\mu}{m}) \left[2v^i v^j - \frac{r^i r^j}{r^2} (2\tilde{E} + \frac{3m}{r} - 3\dot{r}^2) - \frac{4v^{(i} v^{j)} \dot{r}}{r} \right] \\ & + 2 \left\{ (1 - \frac{3\mu}{m}) v^i v^j \tilde{E} - \frac{mr^i r^j}{r^3} \left[3\tilde{E} (1 + \frac{\mu}{m}) - (2 - \frac{4\mu}{m}) \frac{m}{r} - \frac{3\mu \dot{r}^2}{2m} \right] + (4 - \frac{2\mu}{m}) \frac{v^{(i} r^{j)} m \dot{r}}{r^2} \right\} \\ & + (1 - \frac{3\mu}{m}) \left\{ 2(\mathbf{n} \cdot \mathbf{v})^2 (v^i v^j - \frac{mr^i r^j}{3r^3}) - \frac{4m}{3r^3} (\mathbf{n} \cdot \mathbf{v}) (\mathbf{n} \cdot \mathbf{v}) (8v^{(i} r^{j)}) - \frac{3\dot{r} r^i r^j}{r} \right. \\ & \left. - \frac{m}{3r^3} (\mathbf{n} \cdot \mathbf{r})^2 \left[14v^i v^j - \frac{r^i r^j}{r^2} (6\tilde{E} + 13\frac{m}{r} - 15\dot{r}^2) - \frac{30v^{(i} r^{j)} \dot{r}}{r} \right] \right\}, \quad (60) \end{aligned}$$

where $m = m_1 + m_2$, $\mu = m_1 - m_2$, $\dot{r} = \frac{dr}{dt}$, and $\mathbf{r} = r(\cos \phi e_x + \sin \phi e_y)$. Following Wagoner and Will (1975), substituting Equation 60 in Equation 59 and integrating over the solid angle, $d\Omega$, yields a new luminosity equation. The luminosity of a two body system with post-Newtonian corrections to the $O(\epsilon)$ order is:

$$\begin{aligned} L = & \frac{8\mu^2 m^2}{15r^4} \left\{ (12v^2 - 11\dot{r}^2) + 24(\tilde{E} + m/r) \left[\frac{14\mu \tilde{E}}{m} - (6 - 9\mu/m)mr \right] + \dot{r}^2 \left[2\tilde{E}(33 + 43\mu/m) + 3m/r(8 + 21\mu/m) \right. \right. \\ & \left. \left. + \frac{3}{2}(20 + 3\mu/m)\dot{r}^2 + 4(1 - 6\mu/m)[(\tilde{E} + m/r)(6\tilde{E} + 7m/r) - \frac{1}{3}\dot{r}^2(21\tilde{E} + 23m/r - 6\dot{r}^2)] \right. \right. \\ & \left. \left. + \frac{1}{7}(1 - 3\mu/m)[16(\tilde{E} + m/r)(17\tilde{E} - 10m/r) - \frac{1}{3}\dot{r}^2(144\tilde{E} - 440m/r + 105\dot{r}^2)] \right. \right. \\ & \left. \left. + \frac{1}{7}(1 - 4\mu/m)[(\tilde{E} + m/r)(345\tilde{E} + 397m/r) + 4(m/r)^2 - \dot{r}^2(319\tilde{E} + 349m/r - (297\dot{r}^2/4))] \right\}, \quad (61) \end{aligned}$$

where the negative binding energy \tilde{E} is

$$\tilde{E} = \frac{1}{2}v^2 - \frac{m}{r} + \frac{3}{8}v^4(1 - 3\mu/m) + \frac{1}{2}\frac{m^2}{r} + (3v^2m/2r)(1 + \mu/3m) + \frac{\mu}{2r}(\mathbf{v} \cdot \mathbf{r}/r)^2 \quad (62)$$

As noted in Section I, the luminosity is only dependent on initial conditions and the orbital shape of the stellar encounter. Therefore, the general result (61) may be used to calculate the GW luminosity emitted from stellar encounters of various orbital shapes. Substituting $\epsilon = 0$, $\phi = \omega t$, and $\omega = 4J * E^2/m^2$ in Equation 61 we found that the radiation luminosity emitted from a binary system with a circular orbit is consistent with Wagoner and Will's (1975) result [6]:

$$L = \frac{l}{105l^3(l+3m-u)^6} 8mu^2 \left(14\tilde{E}l^3m(15m-116u)(l+3m-u) + \tilde{E}l^3(785m-852u)(l+3m-u)^2 \right. \\ \left. + m^2(42l^4 + 84L(3m-u)^3 - 42l^2(-3m-u)^2 + 84(-3,-u)^4 - l^3(571m+788u)) \right. \\ \left. - 42lm^2(l+3m-u)^2(l-6m+2u) \cos \left[\frac{8\tilde{E}^2Jt}{m^2} \right] \right), \quad (63)$$

where the angular momentum per reduced mass, J is:

$$J = (mp)^{1/2}1 + (m/2p)[(7 - \mu/m) + (1 - 3\mu/m)e^2]. \quad (64)$$

Modeling the GW Waveforms

To model the waveforms of stellar encounters with post-Newtonian corrections it is convenient to represent the strain amplitude in an alternate basis related to θ and ϕ . The observer's line of sight toward the stellar encounter is defined as $n = \sin\theta e_x + \cos\theta e_z$, where θ is the angle between n and the z axis (orthogonal to the plane of the observer). A new basis which is orthogonal to the observer's direction is defined as having the independent components $e_\theta = \frac{1}{R} \frac{\partial}{\partial \theta}$ and $e_\phi = \frac{1}{R \sin\theta} \frac{\partial}{\partial \phi}$ [6]. In this basis the two independent components of the strain $h_{TT}^{\theta\theta} = -h_{TT}^{\phi\phi}$ and $h_{TT}^{\theta\phi}$ can be calculated using Equation 60, where $i, j = \theta, \phi$. The velocity and radius vectors, v^i, r^j , respectively, are given by

$$v = \sqrt{\frac{m}{l}} \left[-\sin\phi e_x + (\epsilon + \cos\phi)e_y + \frac{m}{l} \left\{ e_x \left[-3\epsilon\phi + \left(3 - \frac{\mu}{m}\right)\sin\phi - \left(1 + \frac{21\mu}{8m}\right)\epsilon^2\sin\phi + \frac{1}{2}\left(1 - \frac{2\mu\epsilon}{m}\right)\sin 2\phi - \frac{\mu\epsilon^2}{8m}\sin(3\phi) \right] \right. \right. \\ \left. \left. + e_y \left[-\left(3 - \frac{\mu}{m}\right)\cos\phi - \left(3 - \frac{31\mu\epsilon^2}{8m}\right)\cos(\phi) - \frac{1}{2}\left(1 - \frac{2\mu}{m}\right)\epsilon\cos(2\phi) + \frac{\mu\epsilon^2}{8m}\cos(3\phi) \right] \right\} \right]; \quad (66)$$

$$r = l \left[1 + \epsilon \cos\phi + \frac{m}{l} \left[-\left(3 - \frac{\mu}{m}\right) + \left(1 + \frac{9\mu}{4m}\right)\epsilon^2 + \frac{1}{2}\left(7 - \frac{2\mu}{m}\right)\epsilon\cos\phi + 3\epsilon\phi\sin\phi - \frac{\mu}{4m}\epsilon^2\cos 2\phi \right] \right]^{-1} \quad (67)$$

The components of radius and velocity in the new basis are found by taking the dot product of 66 and 67 with the basis vectors, e_θ and e_ϕ . Using these results we found the general form of the strain in the new basis and substituted different ϵ values to model the gravitational waveforms of stellar encounters with varying orbital shapes.

RESULTS

Since we are mainly interested in the effects of eccentricity on the shape of gravitational waveforms, rather than exact numerical calculations of strain amplitude, we took the physical constants G and c to be 1 and used the parameter values in Table II. We found that for all possible eccentricities, the strain amplitude for the $h_{TT}^{\theta\phi}$ polarization remains constant as ϕ varies. The resulting waveforms for the $h_{TT}^{\phi\phi}$ polarization follow.

Figure 10 shows how drastically changes in ϵ effect the waveforms and maximum amplitudes in the $\phi\phi$ polarization. Comparison of figures 4, 5, and 8 suggest that strain amplitude generally increases as ϵ increases, and increases

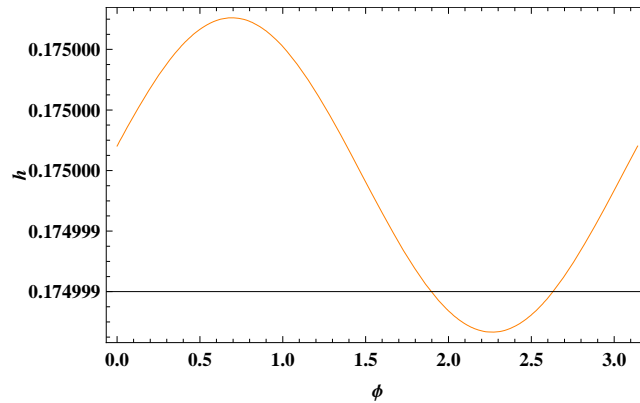


FIG. 4: Gravitational waveforms of circular orbits with $\epsilon = 0$. The angle from the observer to the orbital plane, θ , is $\pi/4$.

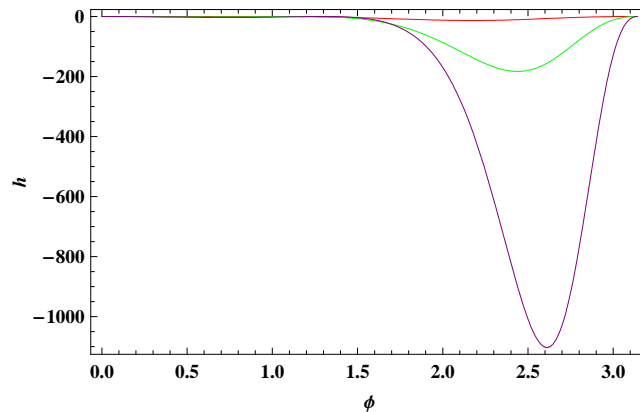


FIG. 5: Gravitational waveforms of elliptical orbits with an eccentricity of $\epsilon = 0.2$ (red), 0.5 (green), 0.7 (purple) where $\theta = \pi/4$.

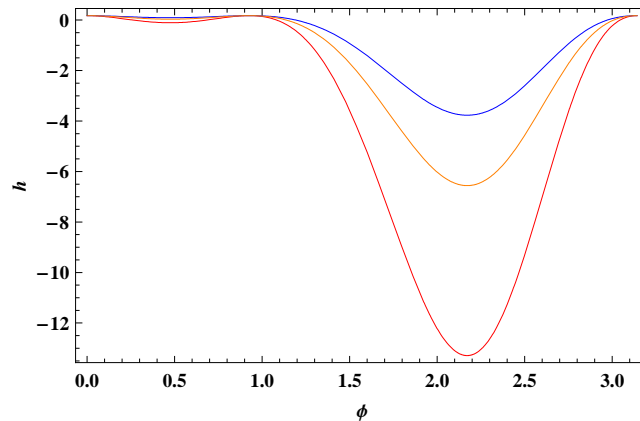


FIG. 6: Gravitational waveforms of elliptical orbits with $\epsilon = 0.2$ as θ varies. The red line represents $\theta = \pi/4$, orange $\theta = \pi/6$, and blue $\theta = \pi/8$.

dramatically when $\epsilon = 1$. The parabolic waveform ($\epsilon = 1$) was omitted from Figure 10 because the maximum amplitude is so much larger than that of the other orbit types that the circular, elliptical, and hyperbolic waveforms are obscured when plotted with the parabolic waveform. While θ has a much smaller effect on strain amplitudes than the eccentricity, Figures 6, 7, and 9 show that larger values of θ yield larger maximum strain amplitudes. Our analysis found that the strain amplitude for the $\theta\phi$ polarization is constantly $2\mu/R$, and has no dependence on θ , ϕ , or ϵ . This could be due to the possibility that in an average over several wavelengths the wave amplitudes can cancel each other

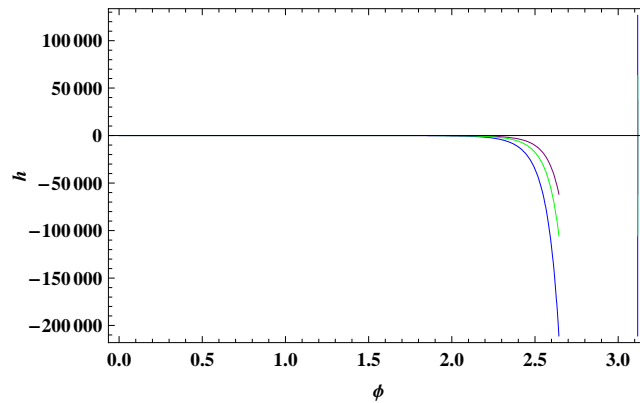


FIG. 7: Gravitational waveforms of parabolic orbits with $\epsilon = 1$ as θ varies. The blue line represents $\theta = \pi/4$, green $\theta = \pi/6$, and purple $\theta = \pi/8$.

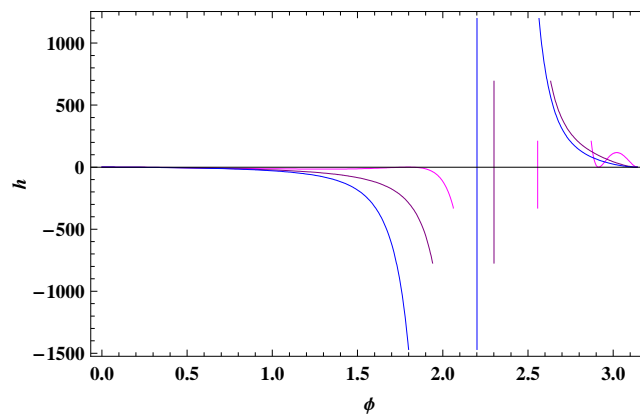


FIG. 8: Gravitational waveforms of hyperbolic orbits with $\theta = \pi/4$. The magenta line represents eccentricity $\epsilon = 1.2$, the purple line $\epsilon = 1.5$, and the blue line $\epsilon = 1.7$.

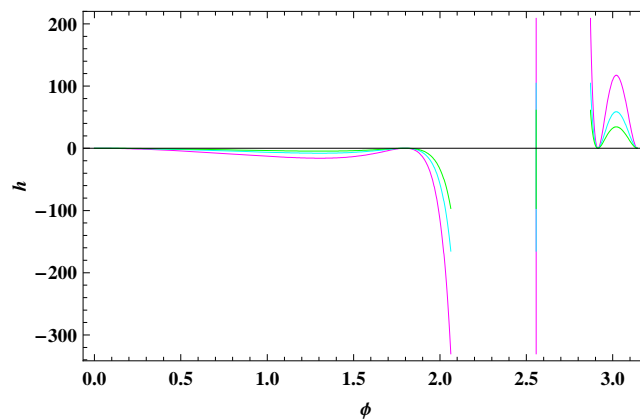


FIG. 9: Gravitational waveforms of hyperbolic orbits with $\epsilon = 1.2$ as θ varies. The magenta line represents $\theta = \pi/4$, cyan $\theta = \pi/6$, and green $\theta = \pi/8$.

out. This possibility should be investigated further in future work to determine the mechanism which leads to the constancy of $h_{TT}^{\theta\phi}$.

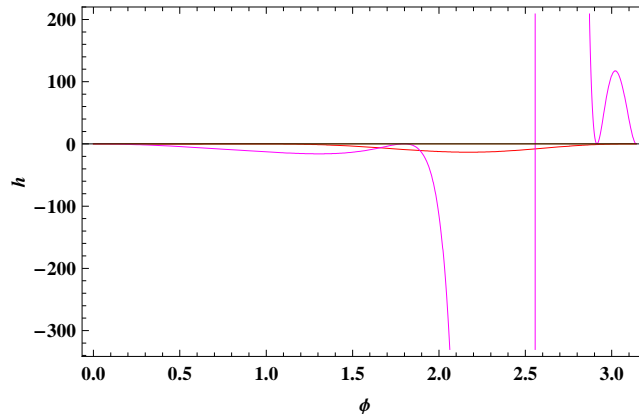


FIG. 10: Gravitational waveforms of varying eccentricities (ϵ) and a constant angle of the observer, $\theta = \pi/4$. The orange line represents a circular orbit with $\epsilon = 0$, red an elliptical orbit ($\epsilon = 0.2$), and magenta a hyperbolic orbit ($\epsilon = 1.2$).

CONCLUSION

Quantifying the amplitudes of waves from different stellar interactions should help identify the source of gravitational waves received by future detectors. While analysis based on classical Newtonian mechanics gives a basic picture of gravitational waveforms from binary stellar encounters, post-Newtonian corrections improve the accuracy of the waveforms by considering higher order relativistic effects. More accurate templates of GWs will help to determine the sources of incoming signals. Our results suggest that the GW amplitude of binary stellar encounters to the $O(\epsilon^2)$ order increase with eccentricity, and jump up sharply for parabolic encounters at $\epsilon = 1$. We also found that eccentricity has a much more pronounced effect on the waveforms and amplitude than the angle of observation, θ . It is important to note that only post-Newtonian corrections introduce this additional dependence on θ at all, while classical solutions depend solely on the initial conditions of the stellar system. The obvious differences demonstrated here between waveforms predicted by a classical approach and post-Newtonian models indicate that to effectively resolve the stochastic signal, processing should use model waveforms which at least account for relativistic corrections.

Modeling gravitational waveforms could prove particularly useful for resolving the sources of GWs in the stochastic background, since it is comprised of signals from many unresolved, uncorrelated sources. Determining whether components of the background are from astrophysical sources such as the stellar interactions explored here or from cosmological sources could yield interesting information about the early universe. Modeling gravitational waveforms in order to analyze the stochastic background is also useful because detectors will receive data from the stochastic background virtually constantly, while GW bursts from events such as black hole collisions have a fairly low incidence rate. Further work could include higher order post-Newtonian corrections which would account for the effects of spin, radiation reaction, and tidal effects, which could all possibly introduce significant changes in models of gravitational waveforms and improve the accuracy of signal processing.

REFERENCES

-
- Abbot, B. et. al. 2007. *Searching for a Stochastic Background of Gravitational Waves with LIGO* *Astrophys. J.* 695: 918-930.
- Allen, B. 1996. *The stochastic gravity-wave background: sources and detection* Proceedings of the Les Houches School on Astrophysical Sources of Gravitational Waves, <http://www.citebase.org/abstract?id=oai:arXiv.org:gr-qc/9604033>.
- Capozziello, S. and M.D. Laurentis, *Gravitational Waves from Stellar Encounters* *Astroparticle Physics*, 30(2008): 1222-1231.
- Epstein, R. and R. V. Wagoner, 1975. *Astrophys. J.* 197, 717.
- Misner, C., K. Thorne, and J. Wheeler. *Gravitation*. W. H. Freeman and Company: 1973.

Wagoner, R. V. and Clifford M. Will, 1976. *Post Newtonian Gravitational Radiation from Orbiting Point Masses*, *Astrophys. J.* 210, 764-775.